

## Article

# Double Photodiode Readout System for the Calorimeter of the HERD Experiment: Challenges and New Horizons in Technology for the Direct Detection of High-Energy Cosmic Rays

Pietro Betti <sup>1,\*</sup> , Oscar Adriani <sup>1</sup> , Matias Antonelli <sup>2</sup> , Yonglin Bai <sup>3</sup> , Xiaohong Bai <sup>3</sup>, Tianwei Bao <sup>4</sup>, Eugenio Berti <sup>5</sup>, Lorenzo Bonechi <sup>5</sup>, Massimo Bonghi <sup>1</sup> , Valter Bonvicini <sup>2</sup>, Sergio Bottai <sup>5</sup>, Weiwei Cao <sup>3</sup> , Jorge Casaus <sup>6</sup> , Zhen Chen <sup>3</sup>, Xingzhu Cui <sup>4</sup>, Raffaello D'Alessandro <sup>1</sup> , Sebastiano Detti <sup>5</sup>, Carlos Diaz <sup>6</sup>, Yongwei Dong <sup>4</sup>, Noemi Finetti <sup>5,7</sup> , Valerio Formato <sup>8</sup> , Miguel Angel Velasco Frutos <sup>6</sup> , Jiarui Gao <sup>3</sup>, Francesca Giovacchini <sup>6</sup>, Xiaozhen Liang <sup>3</sup>, Ran Li <sup>3</sup>, Xin Liu <sup>4,9</sup> , Linwei Lyu <sup>3</sup>, Gustavo Martinez <sup>6</sup> , Nicola Mori <sup>5</sup> , Jesus Marin Munoz <sup>6</sup>, Lorenzo Pacini <sup>5</sup> , Paolo Papini <sup>5</sup> , Cecilia Pizzolotto <sup>2</sup> , Zheng Quan <sup>4</sup>, Junjun Qin <sup>3</sup>, Dalian Shi <sup>3</sup>, Oleksandr Starodubtsev <sup>5</sup>, Zhicheng Tang <sup>4</sup>, Alessio Tiberio <sup>1</sup>, Valerio Vagelli <sup>10,11</sup> , Elena Vannuccini <sup>5</sup>, Bo Wang <sup>3</sup>, Junjing Wang <sup>4</sup>, Le Wang <sup>12</sup>, Ruijie Wang <sup>4</sup>, Gianluigi Zampa <sup>2</sup> , Nicola Zampa <sup>2</sup> , Zhigang Wang <sup>4</sup>, Ming Xu <sup>4</sup>, Li Zhang <sup>4</sup> and Jinkun Zheng <sup>3</sup>

- <sup>1</sup> Dipartimento di Fisica e Astronomia, Università degli Studi di Firenze and INFN Firenze, Via Sansone 1, 50019 Sesto Fiorentino, Italy; adriani@fi.infn.it (O.A.); bonghi@fi.infn.it (M.B.); candi@fi.infn.it (R.D.); tiberio@fi.infn.it (A.T.)
  - <sup>2</sup> INFN Trieste, via Valerio 2, 34127 Trieste, Italy; walter.bonvicini@ts.infn.it (V.B.); cecilia.pizzolotto@ts.infn.it (C.P.); gianluigi.zampa@ts.infn.it (G.Z.); nicola.zampa@ts.infn.it (N.Z.)
  - <sup>3</sup> Xi'an Institute of Optics and Precision Mechanics of CAS, Xi'an 710019, China; baiyonglin@opt.ac.cn (Y.B.); bxh@opt.ac.cn (X.B.); caoweiwei@opt.ac.cn (W.C.); chenzhen@opt.ac.cn (Z.C.); gaojiarui@opt.ac.cn (J.G.); liangxiaozhen@opt.ac.cn (X.L.); liran@opt.ac.cn (R.L.); lvlinwei@opt.ac.cn (L.L.); qjj@opt.ac.cn (J.Q.); lotus@opt.ac.cn (D.S.); wbo@opt.ac.cn (B.W.); zhjink@opt.ac.cn (J.Z.)
  - <sup>4</sup> Institute of High Energy Physics, Chinese Academy of Sciences, Beijing 100049, China; baotw@ihep.ac.cn (T.B.); cuixingzhu@ihep.ac.cn (X.C.); dongyw@ihep.ac.cn (Y.D.); xliu@ihep.ac.cn (X.L.); quanzheng@ihep.ac.cn (Z.Q.); tangzhch@ihep.ac.cn (Z.T.); wangjunjing@ihep.ac.cn (J.W.); wangrj@ihep.ac.cn (R.W.); wangzhg@ihep.ac.cn (Z.W.); mingxu@ihep.ac.cn (M.X.); zhangli@ihep.ac.cn (L.Z.)
  - <sup>5</sup> INFN Firenze, Via Sansone 1, 50019 Sesto Fiorentino, Italy; berti@fi.infn.it (E.B.); lorenzo.bonechi@fi.infn.it (L.B.); bottai@fi.infn.it (S.B.); noemi.finetti@univaq.it (N.F.); mori@fi.infn.it (N.M.); lorenzo.pacini@fi.infn.it (L.P.); papini@fi.infn.it (P.P.); starodubtsev@fi.infn.it (O.S.); vannuccini@fi.infn.it (E.V.)
  - <sup>6</sup> Ciemat, E-28040 Madrid, Spain; jorge.casaus@ciemat.es (J.C.); carlos.diaz@ciemat.es (C.D.); miguelangel.velasco@ciemat.es (M.A.V.F.); francesca.giovacchini@ciemat.es (F.G.); gustavo.martinez@ciemat.es (G.M.); jesus.marin@ciemat.es (J.M.M.)
  - <sup>7</sup> Dipartimento di Scienze Fisiche e Chimiche, Università degli Studi dell'Aquila, Via Vetoio, Coppito, I-67100 L'Aquila, Italy
  - <sup>8</sup> INFN—Sezione di Roma Tor Vergata, via della Ricerca Scientifica 1, I-00133 Roma, Italy; valerio.formato@roma2.infn.it
  - <sup>9</sup> University of Chinese Academy of Sciences, Beijing 101408, China
  - <sup>10</sup> Agenzia Spaziale Italiana, via del Politecnico s.n.c., I-00133 Roma, Italy; valerio.vagelli@asi.it
  - <sup>11</sup> INFN Perugia, Via Alessandro Pascoli 23c, I-06123 Perugia, Italy
  - <sup>12</sup> National Astronomical Observatories, Chinese Academy of Sciences, Beijing 100012, China; wangle@nao.cas.cn
- \* Correspondence: betti@fi.infn.it



**Citation:** Betti, P.; Adriani, O.; Antonelli, M.; Bai, Y.; Bai, X.; Bao, T.; Berti, E.; Bonechi, L.; Bonghi, M.; Bonvicini, V.; et al. Double Photodiode Readout System for the Calorimeter of the HERD Experiment: Challenges and New Horizons in Technology for the Direct Detection of High-Energy Cosmic Rays. *Instruments* **2024**, *8*, 5. <https://doi.org/10.3390/instruments8010005>

Academic Editor: Antonio Ereditato

Received: 12 October 2023

Revised: 13 December 2023

Accepted: 24 December 2023

Published: 22 January 2024



**Copyright:** © 2024 by the authors. Licensee MDPI, Basel, Switzerland. This article is an open access article distributed under the terms and conditions of the Creative Commons Attribution (CC BY) license (<https://creativecommons.org/licenses/by/4.0/>).

**Abstract:** The HERD experiment is a future experiment for the direct detection of high-energy cosmic rays and is to be installed on the Chinese space station in 2027. The main objectives of HERD are the first direct measurement of the *knee* of the cosmic ray spectrum, the extension of electron+positron flux measurement up to tens of TeV, gamma ray astronomy, and the search for indirect signals of dark matter. The main component of the HERD detector is an innovative calorimeter composed of about 7500 LYSO scintillating crystals assembled in a spherical shape. Two independent readout systems of the LYSO scintillation light will be installed on each crystal: the wavelength-shifting fibers system developed by IHEP and the double photodiode readout system developed by INFN and CIEMAT. In order to measure protons in the cosmic ray *knee* region, we must be able to measure energy release of about 250 TeV in a single crystal. In addition, in order to calibrate the system, we need to measure

typical releases of minimum ionizing particles that are about 30 MeV. Thus, the readout systems should have a dynamic range of about  $10^7$ . In this article, we analyze the development and the performance of the double photodiode readout system. In particular, we show the performance of a prototype readout by the double photodiode system for electromagnetic showers as measured during a beam test carried out at the CERN SPS in October 2021 with high-energy electron beams.

**Keywords:** cosmic rays; calorimeters; space instrumentation; large detector systems for particle and astroparticle physics

## 1. Introduction

Direct detection of cosmic rays is limited at high energy by the geometrical acceptance of space experiments. Indeed, the cosmic ray flux decreases with energy as  $E^{-\gamma}$  with  $\gamma \simeq 2.7$ , limiting the number of particles at high energies. Thus, we need experiments with larger acceptances: a feature that contrasts with the high cost per weight of payloads and power consumption availability in space. The HERD (*High Energy cosmic-Radiation Detection facility*) [1,2] experiment is a new experiment for direct detection of high-energy cosmic rays that will be installed on the Chinese space station in 2027. HERD has an innovative design: with mass and power consumption comparable with that of the current experiments in orbit, it will have a very much larger geometric acceptance. Thanks to this, it will expand direct measurement of proton and nuclei fluxes up to the cosmic ray *knee* region (PeV/nucleon) and electron+positron flux up to tens of TeV. Thus, it will expand direct cosmic ray measurements more than one order of magnitude in energy with respect to the current experiments in orbit. In addition, HERD will perform gamma ray astronomy measurements, and with measurement of both electron+positron flux and gamma rays, it will search for indirect signals of dark matter.

The HERD detector is based on an innovative calorimeter geometry: it is surrounded on five faces by sub-detectors for tracking, charge measurement, and an anti-coincidence system. The calorimeter has a spherical shape and is composed of about 7500 three-centimeter cubic LYSO scintillating crystals, as shown in Figure 1. It is homogeneous, finely segmented, 3D, isotropic, and deep (about  $55 X_0$ , and  $3 \lambda_I$ ). The first idea for this type of calorimeter was developed and studied by the CaloCube collaboration, which demonstrated the very large geometric acceptance that can be achieved with this type of space-borne calorimeter [3–8]. Indeed, thanks to its spherical shape, the HERD calorimeter has a very large acceptance. Considering that it is surrounded on five faces by sub-detectors, the experiment can detect particles arriving from five different directions (the only blind face is the one connected to the space station). The calorimeter has good energy resolution: about 2.5% for electromagnetic showers and less than 30% for hadronic showers. In addition, the cubic segmentation permits the 3D-reconstruction of events and good electron–hadron discrimination for particles coming from all directions. Thanks to these features, HERD’s effective geometric factor is about  $2.5 \text{ m}^2 \text{ sr}$  for electrons and about  $1 \text{ m}^2 \text{ sr}$  for protons.

The scintillation light of the LYSO crystals is readout by two independent systems: one based on *Wavelength Shifting Fibers* (WLSFs) coupled to *Intensified scientific CMOS* (IsCMOS) developed by the Chinese Institute of High Energy Physics (IHEP), and the other one based on the use of two photodiodes with different active areas developed by INFN Florence, INFN Trieste, and CIEMAT Madrid. In order to calibrate the readout systems, we need to detect typical energy releases of minimum ionizing particles, which are about 30 MeV, in a crystal. In addition, we want to measure proton and nuclei fluxes up to the PeV/n energies. Since in a single LYSO cube the energy released by PeV/n particles can be as large as 250 TeV, our readout systems must have an extremely high dynamic range: larger than  $10^7$ . Indeed, the saturation level of a single channel is more than 20 times higher than that in current experiments in orbit. In addition, the total number of channels of the HERD

calorimeter will be about 20 times larger than in current calorimeters in orbit [9,10]. These characteristics raise challenges to maintain acceptable power consumption and to manage a higher number of channels.

In this article, we briefly describe the design of the double photodiode readout system. Then, we present the performance studies for electromagnetic showers that were measured on this system during a beam test at CERN SPS in October 2021. Finally, we introduce the new and latest update to the system with some hints about future tests.

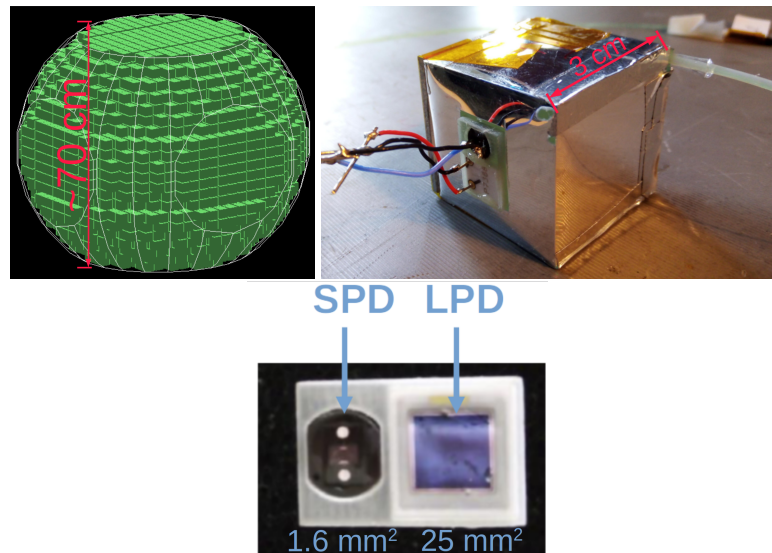


**Figure 1.** **Top left:** scheme of the structure of the calorimeter; about 7500 three-centimeter cubic LYSO crystals are assembled in a spherical shape. **Top right:** picture of a LYSO crystal with WLSF and PD readout systems installed; the crystal is covered with a reflective coating. A monolithic package with photodiodes is glued to front of the crystal. The WLSFs are glued on the top face of the crystal and are placed below a reflective coating; we can see the fibers coming out of the reflective coating in the upper right corner of the image. **Bottom:** an illustration of an in-house-built prototype of a monolithic package for the PD readout system, composed of LPD (*Large PhotoDiode*, 25 mm<sup>2</sup>) and SPD (*Small PhotoDiode*, 1.6 mm<sup>2</sup>).

## 2. The Double Photodiode Read-Out System

The design of the double photodiode readout system is described in detail in [11]. In this section, we recall only the basic elements. The system is based on the use of two photodiodes with different active areas: the *Large PhotoDiode* (LPD), model VTH2110, with an active area of about 25 mm<sup>2</sup>; and the *Small PhotoDiode* (SPD), model VTP9412, with an active area of about 1.6 mm<sup>2</sup>. Both PDs are produced by Excelitas Technologies. The use of PDs with different active areas permits an increase in the dynamic range of the system. Indeed, the LPD is sensitive to small signals that the SPD cannot detect, while the SPD is sensitive to large signals for which the LPD saturates the electronics. The LPD and SPD are glued in a plastic mask to assemble an in-house-built monolithic package (Figure 1). The monolithic package is then fixed with optical glue on a LYSO crystal surface (Figure 1). Finally, the crystal surface is covered by a reflective coating.

The main component of the *front-end electronics* is the HiDRA2 chip, based on the CASIS ASIC [12], that was developed by INFN Trieste specifically for the double photodiode readout system of HERD. The HiDRA2 chip has a high dynamic range (from a few fC to 52.6 pC), low noise, and low power consumption (about 3.73 mW per channel). To reach such a large dynamic range, an automatic gain selector for the *charge-sensitive amplifier* is implemented in the chip: the ratio between *high gain* and *low gain* is about 20. The chips are mounted on the HiDRA board, which is controlled by two other boards: the TROC2 that drives the HiDRA chips and the TROC1 that is the interface between the acquisition PC and the TROC2; the boards are developed by CIEMAT Madrid.

### 3. The SPS2021 Beam Test

#### 3.1. Introduction

In October 2021, we carried out a beam test with a prototype of about 500 LYSO crystals at CERN SPS. Only 63 crystals were equipped with both the double photodiode and WLSF readout systems. The 63 crystals were arranged in 3 columns of 21 crystals each along the beam line (Figure 2), while all the other cubes were equipped with only WLSFs. For a detailed description of the prototype, see [11]. Prototypes of other HERD subsystems (tracker, anti-coincidence, etc.) were installed as well along the beam line upstream of the calorimeter prototype; however, in this article, only the calorimeter data acquired with the PD system are discussed.

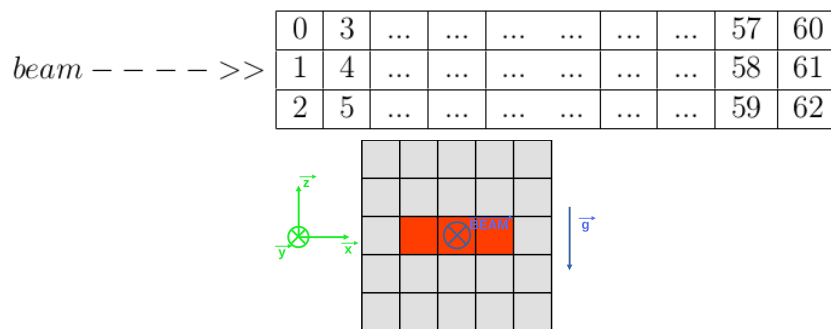


**Figure 2.** **Top:** scheme of the disposition of the crystals equipped with Double Photodiode read-out system, as seen from the sky point of view. **Bottom:** scheme of the crystal distribution in the prototype as seen from the beam’s point of view; the crystals equipped with photodiodes are highlighted in red (the gravity-field direction is shown as reference).

During the beam test, different particle beams were used: muons at 250 GeV; electrons at 50, 100, 150, 200, and 250 GeV; and protons at 350 GeV. The LPDs were calibrated using the energy releases of 250 GeV muons, while the SPDs were calibrated through their correlation with the LPDs using high signals from showers induced by both electrons and protons. The results of the calibration and the characterization of the system during the SPS2021 beam test are discussed in [13]. Subsequently in this article, the energy is expressed in number of MIPs, as explained in [13].

In the following sections, we show the main results of the ongoing analysis of data acquired with the Double Photodiode read-out system for electromagnetic showers. In particular, we discuss the energy resolution and linearity of the calorimeter response for electromagnetic showers. Finally, we show the first measurement of the correlation between the photodiodes and the WLSF signals. In what follows, we consider only the data acquired with the beam hitting the central column of the calorimeter, as shown in Figure 2.

The following results have been reached analyzing only the calorimeter data acquired with the Double Photodiode read-out system. In future, this analysis could be improved using the data from all the detectors on the beam line.

#### 3.2. Energy Resolution for Electromagnetic Showers

We estimate the energy deposited in the calorimeter with two different methods. In the first one, we sum the energy deposited in every crystal, while in the second one, we fit the longitudinal shower profile with a Gamma function. Indeed, the longitudinal profile of the energy deposit for an electromagnetic shower can be parametrized as [14]:

$$\frac{dE}{dt} = E_0 \cdot b \cdot \frac{(b \cdot t)^{a-1} \cdot e^{-b \cdot t}}{\Gamma(a)} \quad (1)$$

where  $E_0$  is the energy of the particle that produced the shower,  $t$  is the length expressed in radiation length ( $X_0$ ),  $a$  and  $b$  are parameters, and  $\Gamma(a)$  is the Euler  $\Gamma$  function. Thus, by

fitting this function to the shower's longitudinal profile, we can estimate the energy of the particle that has induced the shower. An example of this kind of fit is illustrated in Figure 3 (left) for a shower induced by a 250 GeV electron.

The two different estimates of the energy of the particle inducing the shower are compatible within less than 2%; thus, for the remainder of this paper, we consider the reconstructed energy to be the one given by the sum of the energy releases in the crystals.

We study the energy resolution of the calorimeter for electromagnetic showers with electron beams with the energies mentioned in Section 3.1. Considering all the events at the same beam energy, we build a histogram of the total energy release. We perform a fit with a logarithmic Gaussian [14] to estimate the peak position, and we use a confidence level method at 68% to estimate the distribution width. Finally, the energy resolution is given by the ratio between the distribution width and the peak position. In Figure 3 (right), the histogram and the fit result for 100 GeV electrons are shown.

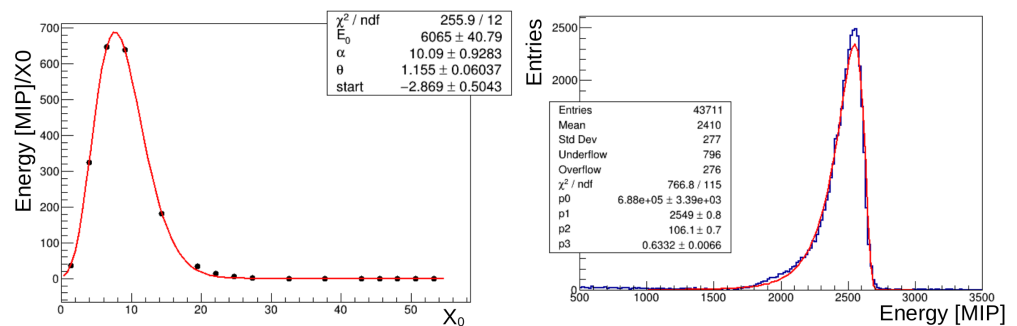


**Figure 3.** Left: fit with a Gamma function of the longitudinal shower profile for a 250 GeV electron shower (note that the energy is expressed in number of MIPs). Right: histogram of the total energy deposits for 100 GeV electron beam fitted with a logarithmic Gaussian.

The energy resolution estimated as a function of the beam energy is reported in Figure 4.

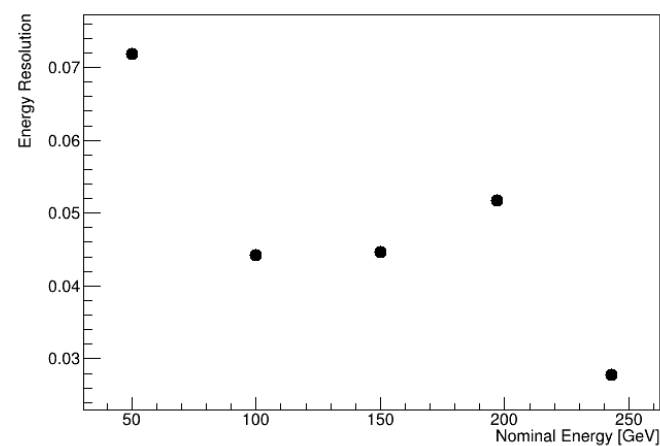


**Figure 4.** Energy resolution of the prototype for electromagnetic showers tested during SPS2021 beam test.

The energy resolution ranges from about 2.5% for 250 GeV electrons up to about 7% for 50 GeV electrons, and it does not monotonically decrease with energy. Instead, by a first Monte Carlo simulation study of the beam test, we expect the energy resolution to monotonically decrease with increasing of the energy from about 3.5% at 50 GeV to about 2.5% at 250 GeV. Thus, the decreases in the performance measured at certain energies are likely due to some experimental effects not implemented in the simulations. By a comparison with the Monte Carlo simulations, we found that if the beam is not parallel

to the y-axis as shown in Figure 2 but is inclined in the yz-plane by less than 0.2 degrees with respect to that axis, it can cause a decrease in the energy resolution up to about 7%. Indeed, in this case, we have a lateral leakage of the shower in the vertical direction (z-axis) since we are considering only data acquired with one tray of crystals, because only one tray was equipped with the double photodiode readout system. Furthermore, inclination of the beam of this entity seems realistic considering the differences in beam shape that we monitored with the beam-line monitor when changing the energy of the electron beam and considering that the alignment procedure of the calorimeter was checked by eye with the help of a laser level, which is a procedure with a precision of a few mm. Finally, with the Monte Carlo simulations, we also checked that inclination with respect to the y-axis but in the xy-plane as compatible with the laser level alignment procedure cannot significantly influence the energy resolution (in this direction, indeed we have three columns of crystals and thus much better shower containment with respect to the z-axis).

### 3.3. Energy Linearity for Electromagnetic Showers

To measure the linearity of the prototype's response to electromagnetic showers, we build a graph, which has on the x-axis the nominal energy of the beam electrons and on the y-axis the energy measured as the sum of the energy releases in the crystals. Then, we perform a linear fit on the graph and estimate the deviation of every point from the fit, as illustrated in Figure 5. We can see in the figure that the non-linearity is less than 3%. This is quite a good result considering that this analysis does not make use of data from other subsystems like the particle tracker, and that due to the geometry of the set of cubes instrumented with PDs and because the beam structures vary with energy, we expect different lateral leakages along the vertical direction that varies with the energy.

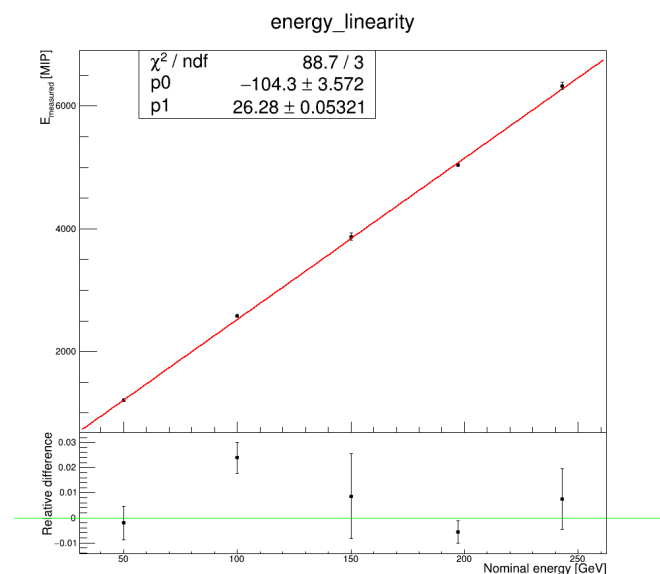


**Figure 5.** Linearity response for electromagnetic showers of the prototype tested during SPS2021 beam test. **Top:** energy measured in the calorimeter as a function of beam energy. The points are fitted with a straight line (red line). **Bottom:** the relative differences between the points and the fit result are plotted (for better visualization a green line corresponding to no differences is plotted).

### 3.4. Double Photodiode and WLSF Read-Out System Correlation

The beam test at SPS2021 is the first beam test in which the two readout systems for the scintillation light of LYSO crystals were completely integrated on the same crystals. Indeed, as described before, the 63 crystals we are considering for this analysis are equipped with both the WLSF and double photodiode readout systems. Thus, this is the first beam test during which we acquired signals induced by high-energy muons, electrons, and protons

in the same crystals with the two independent systems. An example of the correlation of the signals of a crystal acquired with the LPD and with the WLSFs in high and low gain is shown in Figure 6. We clearly see in the figure that the two signals are correlated: this is the first measurement with high-energy particles of this correlation and demonstrates the possibility to use these two independent readout systems to collect light signals on a single cube and to crosscheck each other. The correlation for the single cubes has already proved a valuable tool during the beam test to monitor both the systems and to promptly spot possible problems in one of the two systems.

The correlation analysis was finalized only on single crystals. However in Autumn 2023, we performed a beam test at CERN PS and SPS with a 1000-crystal prototype for which all crystals were equipped with double photodiode and WLSF systems; so we are going to check the correlation between the two readout systems not only for the single cubes alone but also for aggregate variables like the total energy release.

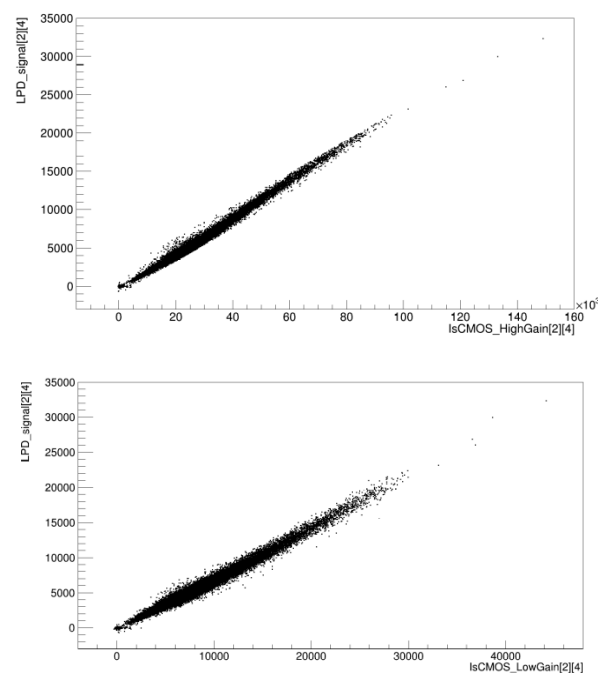


**Figure 6.** Correlation plots for signals acquired in the same crystals by double photodiode and WLSF readout systems. The y-axis shows the signal acquired by the LPD, while x-axis shows the signal acquired by the WLSFs in high gain (top) and in low gain (bottom). Both signals are expressed in ADC units. We clearly see that the two independent readout signals are correlated.

#### 4. Development of a New Monolithic Package for Double Photodiode Read-Out System

As explained in [13], the first homemade prototype of the photodiode system (described in Section 2) does not have the final characteristics needed for the flight detector: indeed, the saturation level of the SPD is about 3.5 TeV instead of about 250 TeV. Therefore, after the characterization, we worked with Excelitas Technologies to produce a new version of the package with a modified SPD in order to reach the desired saturation level. The first project using this new photodiode package has already been presented in [13]. In this new version of the package, the SPD surface is covered with an inconel filter to attenuate the light entering its surface and to meet the requirement for the flight model in terms of maximum detectable energy release. In particular, the optical transmittance of the filter is about 1.5% for [410; 450] nm light, which is the LYSO's peak emission. In addition, LPDs and SPDs are directly assembled in the same FR4 package to form a monolithic package. Indeed, a homemade version of the package is very useful for the prototypal stage, but for the final sensors, we need an industrial version in order to keep the production under strong control and to minimize the variability between the packages. Over the course of

the proceeding year, we finalized this first project and developed the first prototypes: a sketch of the homemade package, the project of the new package, and a prototype of the new package are illustrated in Figure 7.

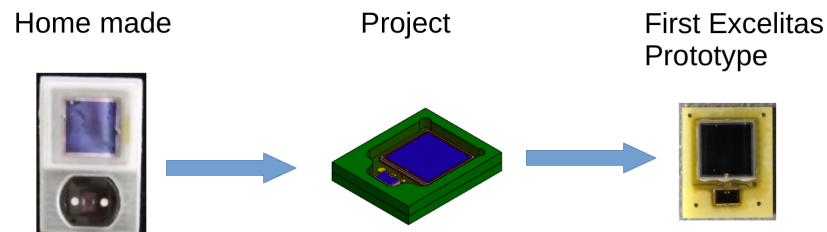


**Figure 7.** Sketch of the passage from the homemade package to the first Excelitas prototype.

This new version of the package has already been mounted on more than 1000 crystals to form a prototype of the calorimeter that was tested at PS and SPS in September and October 2023, respectively (as already mentioned in Section 3.4). All the crystals are equipped with both PD and WLSF systems.

The crystals were installed on 7 trays, every tray containing 7 columns with 21 crystals each. Thus, the prototype had a thickness of about  $55 X_0$  for particles parallel to the columns, as in the flight model. A picture of a tray of the prototype is reported in Figure 8.



**Figure 8.** Picture of the bottom of one calorimeter tray for the prototype that was tested at CERN PS and SPS in September and October 2023. On the right is situated the *front-end electronics* board. The monolithic packages are glued to the crystals and come out from the bottom of the tray through some holes; they are connected to the front-end board via the brown cables that we can see in the figure. Both the cables and the front-end board are specifically designed for the double photodiode readout system.

The prototype was tested with muon, electron, proton, and nuclei beams. With respect to the SPS 2021 beam test, the other sub-detectors were also updated, and we acquired data on a common event-by-event basis. Thus, we have a preliminary kind of flight data type with all the info from every detector, allowing for a deep data analysis of the physics performance of the completed HERD detector.

## 5. Discussion

In this article, we have discussed the analysis of data acquired with a prototype of the HERD calorimeter with the double photodiode readout system at a beam test carried out at SPS in 2021. Specifically, we have analyzed the prototype's performance for electromagnetic showers. The energy resolution ranges from about 2.5% to about 7%. The 2.5% value is a good performance for the calorimeter prototype, while the higher value of the energy resolution is compatible with a small inclination of the beam that causes a lateral leakage of the shower in the vertical direction. With regard to the response linearity for electromagnetic showers, we measured a deviation from linearity of less than 3%, which is quite a good result considering the vertical leakage problem. Anyway, regarding this problem, strong improvement is expected when making use of the particle tracker information and instrumenting more cubes with PDs for better shower containment.

In addition, at the SPS 2021 beam test, we demonstrated the correlation between the WLSF and double photodiode readout systems on a crystal-by-crystal basis, and we

already used this calorimeter feature to crosscheck the two systems. We expect to study the correlation on the full calorimeter using the global shower variables from the Autumn 2023 PS and SPS beam tests data.

The new prototype comprises about 1000 LYSO crystals, which are equipped with a new monolithic package that has been developed in collaboration with Excelitas Technologies. In this package, the LPD and SPD are directly assembled in the same FR4 package, and the SPD surface is covered with an optical filter in order to attenuate the signal and reach the desired dynamic range of the readout system.

In conclusion, with the calorimeter geometry and the double photodiode readout system, we are going to reach the desired calorimeter performance for the detection of electromagnetic showers. Moreover, a new monolithic package has been developed in order to extend the photodiode system's dynamic range. We are in the finalization phase of the system, which, step-by-step, is reaching the desired performance that will let the HERD experiment with its innovative calorimeter directly explore the unexplored high-energy range of cosmic rays up to the *knee* region for protons and nuclei and up to tens of TeV for electrons+positrons.

**Author Contributions:** Conceptualization, O.A., R.D. and J.C.; methodology, P.B., E.B., L.P. and N.M.; software, P.B., E.B., L.P., A.T. and N.M.; validation, P.B., E.B. and L.P.; formal analysis, P.B., E.B. and L.P.; investigation, O.S., P.B., E.B., L.P. and N.M.; resources, Y.B., T.B., W.C., X.C., J.G., R.L., X.L. (Xin Liu), L.L., Z.Q., J.Q., D.S., Z.T., B.W., J.W., R.W., Z.W., M.X., L.Z., J.Z., S.D., G.M., J.M.M., V.F., M.A.V.F., C.P., V.V., S.B., L.B., M.B., N.F., P.P., E.V., M.A., V.B., G.Z., N.Z., X.L. (Xiaozhen Liang), X.B., Z.C., L.W., C.D. and F.G.; data curation, P.B., E.B. and L.P.; writing—original draft preparation, P.B.; writing—review and editing, P.B. and N.M.; visualization, P.B. and L.P.; supervision, R.D.; project administration, O.A. and Y.D. All authors have read and agreed to the published version of the manuscript.

**Funding:** Grant No. 12027803 of the National Natural Science Foundation of China.

**Data Availability Statement:** The datasets presented in this article are not readily available because the data access is restricted to the members of the HERD collaboration. Requests to access the datasets should be directed to the authors.

**Conflicts of Interest:** The authors declare no conflicts of interest.

## References

1. HERD The High Energy Cosmic Radiation Detection Facility. Available online: <http://herd.ihep.ac.cn/> (accessed on 27 July 2022).
2. Pacini, L.; Adriani, O.; Bai, Y.L.; Bao, T.W.; Berti, E.; Bottai, S.; Cao, W.W.; Casaus, J.; Cui, X.Z.; D'Alessandro, R.; et al. Design and expected performances of the large acceptance calorimeter for the HERD space mission. In Proceedings of the 37th International Cosmic Ray Conference—PoS(ICRC2021), Berlin, Germany, 12–23 July 2021.
3. Vannuccini, E.; Adriani, O.; Agnesi, A.; Albergo, S.; Auditore, L.; Basti, A.; Berti, E.; Bigongiari, G.; Bonechi, L.; Bonechi, S.; et al. CaloCube: A new-concept calorimeter for the detection of high-energy cosmic rays in space. *Nucl. Instrum.* **2017**, *845*, 421–424. [[CrossRef](#)]
4. Adriani, O.; Agnesi, A.; Albergo, S.; Auditore, L.; Basti, A.; Berti, E.; Bigongiari, G.; Bonechi, L.; Bonechi, S.; Bongi, M.; et al. Calocube—A highly segmented calorimeter for a space based experiment. *Nucl. Instrum.* **2016**, *824*, 609–613.
5. Bongi, M.; Adriani, O.; Albergo, S.; Auditore, L.; Bagliesi, M.G.; Berti, E.; Bigongiari, G.; Boezio, M.; Bonechi, L.; Bonechi, S.; et al. CALOCUBE: An approach to high-granularity and homogeneous calorimetry for space based detectors. *J. Phys. Conf. Ser.* **2015**, *587*, 012029. [[CrossRef](#)]
6. Pacini, L.; Adriani, O.; Agnesi, A.; Albergo, S.; Auditore, L.; Basti, A.; Berti, E.; Bigongiari, G.; Bonechi, L.; Bonechi, S.; et al. CaloCube: An innovative homogeneous calorimeter for the next-generation space experiments. *J. Phys. Conf. Ser.* **2017**, *928*, 012013. [[CrossRef](#)]
7. Adriani, O.; Albergo, S.; Auditore, L.; Basti, A.; Berti, E.; Bigongiari, G.; Bonechi, L.; Bonechi, S.; Bongi, M.; Bonvicini, V.; et al. CaloCube: An isotropic spaceborne calorimeter for high-energy cosmic rays. Optimization of the detector performance for protons and nuclei. *Astropart. Phys.* **2017**, *96*, 11–17. [[CrossRef](#)]
8. Berti, E.; Adriani, O.; Albergo, S.; Ambrosi, G.; Auditore, L.; Basti, A.; Bigongiari, G.; Bonechi, L.; Bonechi, S.; Bongi, M.; et al. CaloCube: A new concept calorimeter for the detection of high energy cosmic rays in space. *J. Phys. Conf. Ser.* **2019**, *1162*, 012042. [[CrossRef](#)]
9. Chang, J.; Ambrosi, G.; An, Q.; Asfandiyarov, R.; Azzarello, P.; Bernardini, P.; Bertucci, B.; Cai, M.S.; Caragiulo, M.; Chen, H.F.; et al. The DArk Matter Particle Explorer mission. *Astropart. Phys.* **2017**, *95*, 6–24. [[CrossRef](#)]

10. Torii, S. The CALorimetric Electron Telescope (CALET): High Energy Astroparticle Physics Observatory on the International Space Station. In Proceedings of the 34th International Cosmic Ray Conference—PoS(ICRC2015), The Hague, The Netherlands, 30 July–6 August 2015.
11. Adriani, O.; Antonelli, M.; Basti, A.; Berti, E.; Betti, P.; Bigongiari, G.; Bonechi, L.; Bongi, M.; Bonvicini, V.; Bottai, S.; et al. Development of the photo-diode subsystem for the HERD calorimeter double-readout. *JINST* **2022**, *17*, P09002. [[CrossRef](#)]
12. Bonvicini, V.; Orzan, G.; Zampa, G.; Zampa, N. A Double-Gain, Large Dynamic Range Front-end ASIC with A/D Conversion for Silicon Detectors Read-Out. *IEEE Trans. Nucl. Sci.* **2010**, *57*, 2963–2970. [[CrossRef](#)]
13. Betti, P.; Adriani, O.; Antonelli, M.; Bai, Y.; Bai, X.; Bao, T.; Berti, E.; Bonechi, L.; Bongi, M.; Bonvicini, V.; et al. Photodiode Read-Out System for the Calorimeter of the Herd Experiment. *Instruments* **2022**, *6*, 33. [[CrossRef](#)]
14. Grupen C.; Shwartz B. *Particle Detectors*, 2nd ed.; Cambridge Monographs on Particle Physics, Nuclear Physics and Cosmology; Cambridge University Press: Cambridge, UK, 2008; pp. 230–272.

**Disclaimer/Publisher’s Note:** The statements, opinions and data contained in all publications are solely those of the individual author(s) and contributor(s) and not of MDPI and/or the editor(s). MDPI and/or the editor(s) disclaim responsibility for any injury to people or property resulting from any ideas, methods, instructions or products referred to in the content.